BIOPHARMACEUTICS & DRUG DISPOSITION
Biopharm. Drug Dispos. **33**: 99–110 (2012)
Published online 4 March 2012 in Wiley Online Library
(wileyonlinelibrary.com) **DOI**: 10.1002/bdd.1771

Review

Utility of a physiologically–based pharmacokinetic (PBPK) modeling approach to quantitatively predict a complex drug–drug–disease interaction scenario for rivaroxaban during the drug review process: implications for clinical practice

Joseph A. Grillo[a], Ping Zhao[a,*], Julie Bullock[a], Brian P. Booth[a], Min Lu[b], Kathy Robie-Suh[b], Eva Gil Berglund[c], K. Sandy Pang[d], Atiqur Rahman[a], Lei Zhang[a], Lawrence J. Lesko[a], and Shiew-Mei Huang[a]

[a]*Office of Clinical Pharmacology, Office of Translational Sciences, Center for Drug Evaluation and Research, U.S. Food and Drug Administration, Silver Spring, MD, USA*

[b]*Division of Hematology Products (DHP), Center for Drug Evaluation and Research, U.S. Food and Drug Administration, Silver Spring, MD, USA*

[c]*Medical Products Agency, Uppsala, Sweden*

[d]*Leslie Dan Faculty of Pharmacy, University of Toronto, Canada*

ABSTRACT: *Background:* Rivaroxaban is an oral Factor Xa inhibitor. The primary objective of this communication was to quantitatively predict changes in rivaroxaban exposure when individuals with varying degrees of renal impairment are co-administered with another drug that is both a P-gp and a moderate CYP3A4 inhibitor. *Methods*: A physiologically based pharmacokinetic (PBPK) model was developed to simulate rivaroxaban pharmacokinetics in young (20–45 years) or older (55–65 years) subjects with normal renal function, mild, moderate and severe renal impairment, with or without concomitant use of the combined P-gp and moderate CYP3A4 inhibitor, erythromycin. *Results*: The simulations indicate that combined factors (i.e., renal impairment and the use of erythromycin) have a greater impact on rivaroxaban exposure than expected when the impact of these factors are considered individually. Compared with normal young subjects taking rivaroxaban, concurrent mild, moderate or severe renal impairment plus erythromycin resulted in 1.9-, 2.4- or 2.6-fold increase in exposure, respectively in young subjects; and 2.5-, 2.9- or 3.0-fold increase in exposure in older subjects. *Conclusions*: These simulations suggest that a drug–drug–disease interaction is possible, which may significantly increase rivaroxaban exposure and increase bleeding risk. These simulations render more mechanistic insights as to the possible outcomes and allow one to reach a decision to add cautionary language to the approved product labeling for rivaroxaban. Copyright © 2012 John Wiley & Sons, Ltd.

Key words: Complex drug interactions; renal impairment; physiologically-based pharmacokinetic modeling (PBPK)

*Correspondence to: Office of Clinical Pharmacology, Office of Translational Sciences, U.S. Food and Drug Administration, Silver Spring, MD, USA.
E-mail: ping.zhao@fda.hhs.gov

Preliminary results of PBPK model development were presented in poster and abstract form at the 111th annual meeting of the American Society for Clinical Pharmacology and Therapeutics, Atlanta, GA, March 17–20, 2010; however, the conclusions regarding erythromycin were not presented.

This case was also presented as a brief summary as part of a case series on the use of PBPK modeling in regulatory review at FDA (Zhao P, *et al. Clin Pharmacol Ther* 2011; advance online publication 29 December 2010. doi:10.1038/clpt.2010.298).

The publisher or recipient acknowledges right of the U.S. government to retain a nonexclusive, royalty-free license in and to any copyright covering the article.
The views expressed herein are independent work and do not necessarily represent the views of the U.S. Food and Drug Administration.

Abbreviations: $C_{h,u}$, unbound drug concentration in the liver; C_h, C_{gut}, and C_{pv}, total drug concentrations in the liver, gut, and portal vein; $CL_{filtration}$, filtration clearance; $CL_{int,H}$, hepatic unbound intrinsic clearance; $CL'_{int,H}$, hepatic intrinsic clearance; $CL'_{sec,K}$, plasma renal clearance by net secretion; BP, blood/plasma concentration ratio; CL_p/F, apparent plasma clearance; CL_R, renal clearance; f_A, fraction absorbed; f_b, the unbound fraction in the blood; f_G, fraction bioavailability across gut wall; f_p, unbound fraction in plasma; GFR, glomerular filtration rate; K_a, absorption rate constant; K_{deg}, first order degradation rate constant; K_i,

Received 18 October 2011
Revised 8 January 2012
Accepted 12 January 2012

Copyright © 2012 John Wiley & Sons, Ltd.

reversible inhibition constant; K_I, inhibitor concentration causing half maximal inactivation for time-dependent inhibition; k_{inact}, maximal inactivation rate constant; KP_h, liver/plasma tissue partitioning ratio; KP_k, kidney/plasma tissue partitioning ratio; Q_{ha}, Q_{hv}, and Q_{pv}, hepatic blood flows of hepatic artery, hepatic vein, and portal vein; V_h, V_{gut}, and V_{pv}, volume of the liver, gut lumen and portal vein, and V_{pv} uses plasma as reference; V_{ss}, total plasma volume of distribution at steady state

Introduction

Rivaroxaban (Xarelto®, Janssen Pharmaceuticals, Inc., Titusville, NJ) [1] is an orally administered inhibitor of Factor X_a of the coagulation cascade. It was initially approved in 2011 by the United States (US) Food and Drug Administration (FDA) for the prophylaxis of deep vein thrombosis (DVT), which may lead to pulmonary embolism (PE) in patients undergoing knee or hip replacement surgery [2]. Rivaroxaban was also approved by the European Medicines Agency (EMA) in 2008 for a similar indication [3,4].

Rivaroxaban exhibits complete oral bioavailability (F) for the US approved 10 mg tablet form, and has a low oral clearance (CL/F) (approximately 10 l/h) and an modest volume of distribution (< 1 l/kg) [1,5]. Liver metabolism and kidney excretion account for approximately 60% and 40% of the elimination of rivaroxaban, respectively [1,5–8]. In the liver, cytochrome P450 enzymes (CYPs) CYP3A, CYP2J2, and hydrolytic enzymes each contribute approximately one-third of the hepatic metabolism of rivaroxaban [1,5–8]. Approximately 12% of the metabolites have not been identified. In addition, passive glomerular filtration and active secretion mediated by transporters (likely P-glycoprotein, P-gp and/or breast cancer resistance protein, [1,5,9]) contribute to rivaroxaban renal clearance (CL_R) at a ratio of 1:5 [1,5]. The clearance of rivaroxaban appears to decrease in the elderly [1,5,10].

Increasing rivaroxaban exposure is associated with a steep increase in the risk of major bleeding which makes identification of patient factors, intrinsic and/or extrinsic, that affect exposure to be of great importance [1,4,5]. Figure 1 summarizes the clinically evaluated intrinsic or extrinsic factors that are associated with rivaroxaban exposure change. The US approved product labeling (PI) for rivaroxaban states its use should be avoided in the presence of (i) any hepatic disease with coagulopathy and clinically relevant bleeding risk, (ii) moderate hepatic impairment (Child Pugh B), (iii) severe hepatic impairment (Child Pugh C), (iv) severe renal impairment (creatinine clearance (CL_{cr}) approximately 15–29 ml/min), and (v) co-administration with a combined P-gp and strong CYP3A4 inhibitor (e.g. ketoconazole) unless clinical data suggest a change in exposure is unlikely to affect the bleeding risk [2]. The increased exposure of rivaroxaban in subjects with mild to moderate renal impairment (CL_{cr} 30–80 ml/min) or with a moderate CYP3A/P-gp inhibitor (e.g. erythromycin) did not warrant avoidance or dose modification [2]. However, since rivaroxaban is eliminated both by hepatic metabolism and renal excretion, the issue of complex drug–drug interactions (DDI) involving both of these pathways became a concern of the FDA and the EMA [2,3]. Specifically, patients with any degree of renal impairment with concurrent use of P-gp and weak to moderate CYP3A4

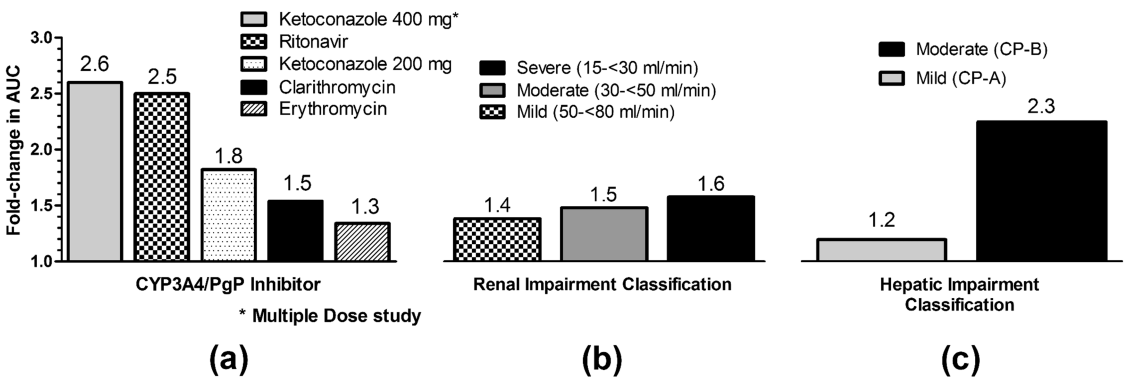

Figure 1. Summary of EMA review of fold changes in exposure (*AUC*) in the presence of (a) CYP3A4/P-gp inhibition compared with no inhibition, (b) various degrees of renal impairment compared with normal renal function and (c) hepatic impairment (Child-Pugh A and B for mild and moderate hepatic impairment, CP-A and CP-B) compared with normal hepatic function

Copyright © 2012 John Wiley & Sons, Ltd.

DOI: 10.1002/bdd

inhibitors may have significant increases in exposure which may increase the bleeding risk [2,3].

The primary objective of this study was to quantitatively evaluate changes in rivaroxaban exposure in individuals when erythromycin is co-administered in subjects with varying degrees of renal impairment using a physiologically based pharmacokinetic (PBPK) modeling and simulation approach.

Materials and Methods

General PBPK model building

The PBPK models of rivaroxaban and erythromycin were developed and used to simulate the pharmacokinetic (PK) profile for rivaroxaban with and without erythromycin in humans. A semi-PBPK model was chosen for rivaroxaban because its human pharmacokinetic profile exhibits an apparent one compartmental distribution behavior [11]. In contrast to a 'full' PBPK model in which organs and tissues are separately represented, a 'semi' PBPK model combines tissues having similar drug partitioning and distribution equilibrium with the plasma compartment [12]. These semi-PBPK models have been utilized to study the dynamics or time-based characteristics of drug–drug interactions [13–15]. A semi-PBPK model was also constructed for erythromycin.

The PBPK model for each compound was composed of a physiological (system-dependent) component and a drug-dependent component [16,17]. Most drug data available in the literature are based on plasma determinations. Hence, our efforts are centered on the utilization of published information from plasma to relate to blood flow, after conversion of the plasma concentration and parameters (the apparent plasma volume of distribution at steady state V_{ss}, and systemic clearances, CL) to blood concentrations and parameters based on the blood to plasma concentration ratio, BP. The physiological component includes the gut compartment, a hypothetical portal vein compartment, the liver and an apparent plasma compartment (Figure 2). In the apparent plasma compartment, drug is assumed to homogenously distribute in all tissues other than the liver and intestines, and it can be eliminated by non-hepatic pathways such as the kidneys. The

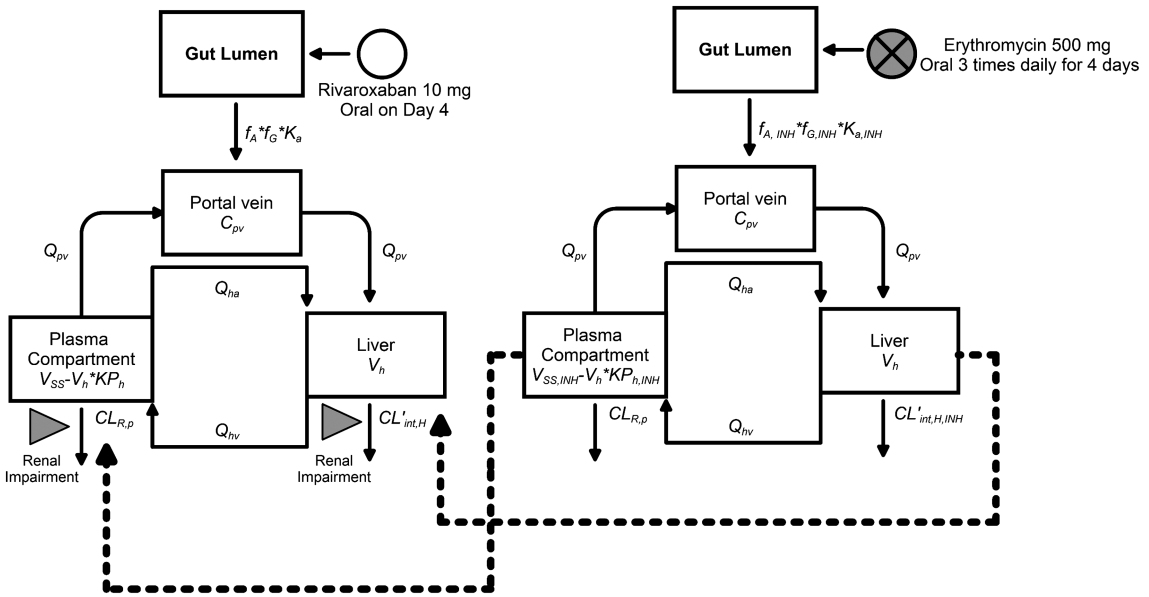

Figure 2. PBPK models of rivaroxaban and enzyme/transporter inhibitor. The inhibitor is either ketoconaozle or erythromycin. Abbreviations are described in Tables 1 and 2. Subscript "inh" denotes inhibitor for the drug-dependent parameters. Solid arrows indicate drug transfer between compartments, either via blood flows (e.g. Q_{pv}, in l/h) or first order transfer (e.g. K_a, in h^{-1}), and the irreversible loss by clearances (CL_R and CL_H). Dashed lines link the inhibitor concentration in the liver and apparent plasma compartments as the operating concentrations for the inhibition effects toward CL_H and CL_R of rivaroxaban, respectively. The volume of distribution of the plasma compartment is described as the difference between the total plasma volume of distribution at steady state (V_{ss}) and the apparent volume of distribution of the liver (referenced to plasma, where V_h and K_{Ph} represent liver volume and the liver:plasma partitioning ratio). ► indicates elimination processes that can be affected by renal impairment

Copyright © 2012 John Wiley & Sons, Ltd.

DOI: 10.1002/bdd

drug-dependent component includes parameters necessary to describe the absorption, distribution, metabolism and excretion (ADME) of the drugs. In both rivaroxaban and erythromycin models, the drug molecule dosed in the gut compartment is absorbed into a hypothetical portal vein compartment of volume V_{pv}. The drug enters the liver compartment by blood flow of the portal vein (Q_{pv}). In the liver, the drug is eliminated by drug metabolizing enzymes or is delivered from the liver compartment to an apparent plasma compartment by blood flow of the hepatic vein (Q_{hv}). Finally, the drug is transferred from the apparent plasma compartment to the liver via blood flows of the hepatic artery (Q_{ha}) and portal vein. That is, $Q_{hv} = Q_{pv} + Q_{ha}$. The dynamics of drug–drug interaction is accomplished by linking the concentration of erythromycin, a combined P-gp and moderate CYP3A4 inhibitor, via appropriate interaction mechanisms within the compartment of interest (see below).

comprising hepatic and renal contributions (CL_H and CL_R) as outlined in Table 1. Geometric mean plasma rivaroxaban concentration versus time data from the literature [11] were digitized (GetData software, Version 2.24, Digital River Inc., Cologne, Germany). The data were fitted to a one-compartment model to estimate K_a using WinNonlin software (V5.2, Pharsight Corp, Cary, North Carolina, USA). The product of the fraction absorbed (f_A) and bioavailability across the gut wall (f_G) was assumed to be 1, based on the high oral bioavailability of nearly 100% for rivaroxaban [1,4]. Although rivaroxaban is tested to be a P-gp substrate *in vitro*, the impact of P-gp on oral absorption of rivaroxaban is considered insignificant because of its complete oral bioavailability. The mass balance rate equations for rivaroxaban in each of the following compartments are expressed by Equations (1–4).

$$\text{Gut compartment} \quad V_{gut}\frac{dC_{gut}}{dt} = -K_a V_{gut} C_{gut} \tag{1}$$

$$\text{Portal vein blood compartment} \quad V_{pv}\frac{dC_{pv}}{dt} = f_A K_a V_{gut} C_{gut} + Q_{pv} C_p BP - Q_{pv} C_{pv} BP \tag{2}$$

$$\text{Liver compartment} \quad V_h\frac{dC_h}{dt} = Q_{pv} C_{pv} BP + Q_{ha} C_p BP - Q_{hv} BP(C_h/KP_h) - CL_{\text{int},H} C_{h,u} \tag{3}$$

$$\text{Apparent plasma compartment} \quad (V_{ss} - V_h KP_h)\frac{dC_p}{dt} = \left[Q_{hv}(C_h/KP_h) - (Q_{pv} + Q_{ha})C_p\right]BP - [f_p GFR + \text{CL}'_{\text{sec},K}]C_p \tag{4}$$

Rivaroxaban PBPK model

The PBPK model was customized to incorporate drug-dependent parameters estimated from human plasma pharmacokinetic studies [11], including the first order absorption rate constant (K_a) describing drug transfer from the gut compartment to the portal vein compartment, V_{ss}, and CL where KP_h is the liver to plasma partitioning ratio. The hepatic intrinsic clearance $CL'_{\text{int,H}}$ is derived from the equation below according to the well-stirred model with hepatic, plasma clearance (CL_H) and upon conversion of CL_H to the hepatic blood clearance, or CL_H/BP, for

Copyright © 2012 John Wiley & Sons, Ltd.

DOI: 10.1002/bdd

Table 1. Physiological and drug-dependent parameters of the PBPK model for the study of rivaroxaban pharmacokinetics

Parameter	Value (unit)	Reference
Physiological		
Q_{hv}	98 (l/h)	[15]
Q_{ha}	24 (l/h)	[15]
Q_{pv}	74 (l/h)	[15]
V_{pv}	0.07 (l)	[15]
V_h	1.87 (l)	[24] See Materials and Method
Age range	Younger: 20–45 (years) Older: 55–65 (years)	[24] See Materials and Method
Weight	Younger: 78.8 (kg) Older: 78.0 (kg)	[24] See Materials and Method
GFR	Younger: 7.63 (l/h) Older: 5.74 (l/h)	[24] See Materials and Method
Rivaroxaban		
K_a	0.75 (1/h)	Estimated using compartmental analysis of phase I data
$f_A{*}f_G$	1	Assumed
Plasma V_{ss}	Young: 48.9 (l) Elderly: 48.4 (l)	[4,9]
f_p	0.065	[4,9]
BP	0.71	[4,9]
KP_h	0.588	Calculated based on physico-chemical properties using SimCYP
$CL_{R,P}$	Young: 4.7 (l/h) Elderly: 2.6 (l/h)	[4,6,9]
CL_H	Younger: 6.0 (l/h) Older: 5.9 (l/h)	[4,6,9]
$f_{m,CYP3A}$ of $CL_{int,H}$	0.37	[4,9]
$f_{m,CYP2J2}$ of $CL_{int,H}$	0.29	[4,9]
$f_{m,other}$ of $CL_{int,H}$	0.34	[4,9]

Q_{hv}, blood flow in hepatic vein; Q_{ha}, blood flow in hepatic artery; Q_{pv}, blood flow in portal vein; V_{pv}, plasma volume of portal vein; V_h, volume of liver; GFR, glomerular filtration rate; K_a, absorption rate constant; f_A, fraction absorbed; f_G, fraction bioavailability across gut wall; V_{ss}, plasma volume of distribution at steady state; $CL_{filtration}$, filtration clearance; BP, blood/plasma concentration ratio; KP_h, liver/plasma tissue partition coefficient; CL_R, plasma renal clearance; CL_H, plasma hepatic clearance; f_m, fractional metabolism in liver.

highly permeable drugs (no transport barrier) [18].

$$CL'_{int,H} = f_b CL_{int,H} = \frac{(CL_H/BP)Q_{hv}}{Q_{hv} - (CL_H/BP)} \quad (5)$$

where f_b is the unbound fraction in the blood (or f_p/BP, Table 1), and $CL_{int,H}$ or the metabolic intrinsic clearance in the liver operates on the unbound concentration in liver $C_{h,u}$ to provide the rate of metabolism. Values of the fractional metabolism (f_m) for CYP3A, CYP2J2, and non-CYP pathways are further found from published literature on rivaroxaban (Table 1). For the apparent plasma compartment, the apparent volume of distribution equals whole body blood volume of distribution (V_{ss}/BP) minus the apparent volume of distribution of rivaroxaban in the liver (reference to blood, $V_h{*}KP_h/BP$). Drug elimination by the kidney is assigned to the apparent plasma compartment. Plasma renal clearance (CL_R) comprises filtration ($CL_{filtration}$, calculated as f_p multiplied by glomerular filtration rate, GFR) and net active secretion ($CL'_{sec,k}$), assumed to be based on plasma drug concentration.

$$CL_R = f_p GFR + CL'_{sec,K} \quad (6)$$

Since transporter mediated active transport in the kidney can result in both secretion and reabsorption, the net active secretion is calculated as the difference between absolute secretion and absolute reabsorption.

PBPK model for erythromycin and coupling of drug models via CYP3A4/P-gp inhibition

The effects of CYP3A4/P-gp inhibition on renal clearance and hepatic clearance of rivaroxaban were incorporated into the PBPK model. The structure of the inhibition model design and relevant equations have been presented elsewhere

Copyright © 2012 John Wiley & Sons, Ltd.

DOI: 10.1002/bdd

Table 2. Drug-dependent parameters of erythromycin used in the PBPK models

Parameter	Value (unit)	Reference
Erythromycin		
$K_{a,Inh}$	0.26 (1/h)	SimCYP Library[a]
$f_{A,Inh} * f_{G,Inh}$	1	Assumed
$V_{ss,Inh}$	Young: 100.1 (l) Elderly: 99.1 (l)	SimCYP Library[a]
$f_{p,Inh}$	0.31	SimCYP Library[a]
$BP_{,Inh}$	0.854	SimCYP Library[a]
Hepatic uptake	1	SimCYP Library[a]
$KP_{h,\ Inh}$	2.71	SimCYP Library[a]
$KP_{k\ Inhplasma}$	2.23	SimCYP Library[a]
$CL_{Inh}\ /F$	63.6 (l/h)	SimCYP Library[a]
$CL_{R,P,Inh}$	3.13 (l/h)	SimCYP Library[a]
$K_{deg,CYP3A4}$	0.03 (h^{-1})	[36]
k_{inact} (CYP3A4)	1.02 (h^{-1})	[37]
K_I	1.48 (μM)	[37]
K_i (CYP2J2)	2 (μM)	Assumed, [35]
K_i ($CL'_{sec,K}$)	11 (μM)	[19]

K_a, absorption rate constant; f_A, fraction absorbed; f_G, fraction bioavailability across gut wall; V_{ss}, total plasma volume of distribution at steady state; $CL_{filtration}$, filtration clearance; BP, blood/plasma concentration ratio; KP_h, liver/plasma tissue partitioning ratio; KP_k, kidney/plasma tissue partitioning ratio; CL_p/F, apparent plasma clearance; $CL_{R,inh}$, renal clearance of inhibitor; K_i, reversible inhibition constant; K_{deg}, 1st order degradation rate constant; k_{inact}, maximal inactivation rate constant; K_I, inhibitor concentration causing 50% maximal inactivation for time-dependent inhibition.

[a]References for SimCYP compound profile 'sim-erytromycin' were: f_p: Dette *et al.*, 1982; [38]; V_{ss} and CL data: Austin *et al.*, 1980; Barre *et al.*, 1982, Josefsson, 1982 [39–41].

[15]. Unless otherwise stated, drug-dependent parameters for erythromycin were extracted from the compound library of the PBPK modeling and simulation software SimCYP® (SimCYP Ltd, Sheffield, UK) (Table 2).

The PBPK models of rivaroxaban and erythromycin are linked such that the effect of the inhibitor on the elimination of rivaroxaban in the liver and the kidney can be simulated in a dynamic fashion (see Figure 2). The inhibition of rivaroxaban elimination pathways via CYP2J2 and renal secretion by efflux transporters was assumed reversible, whereas the inhibition of CYP3A4 was assumed to be time-dependent. The effect of erythromycin on $CL'_{int,H}$ of rivaroxaban is described in Equation (7).

For Equation (7), $f_{m,CYP3A} + f_{m,CYP2J2} + f_{m,non\text{-}CYP} = 1$; $[I]$ is operating inhibitor concentration (see below), and K_i is the reversible inhibition constant, $K_{deg,CYP3A}$ is the apparent first order degradation rate constant of CYP3A, and K_{obs} is the apparent inactivation rate constant in the presence of erythromycin according to Equation (8).

$$K_{obs} = \frac{k_{inact}[I]}{K_I + [I]} \tag{8}$$

In Equation (8), k_{inact} and K_I are maximal inactivation rate constant and inhibitor concentration causing 50% maximal inactivation for time-dependent inhibition of CYP3A, respectively (see Table 3).

As stated earlier, the inhibition effect of erythromycin on $CL'_{sec,K}$ assumes competitive inhibition. For erythromycin, a K_i value of 11 μM was derived from an in vitro study using digoxin as a substrate ($IC_{50} = 22.7$ μM) in Caco-2 cells [19].

Time-based unbound tissue concentrations ($[I]_{u,tissue}$) were used as the operating inhibitor concentrations of erythromycin. Simulations were further conducted to evaluate rivaroxaban pharmacokinetics in subjects with varying degrees of renal impairment (RI).

Effect of RI on the rivaroxaban PBPK model

Both CL_R and CL_H of rivaroxaban were found to be decreased in subjects with varying degrees of renal impairment [20]. The value of CL_R reported for subjects with normal renal function (control group) was 2.4 l/h [20] , a value that is lower than that reported in phase I pharmacokinetic studies (4.7 l/h, Table 1). The renal filtration ($CL_{filtration}$ = mean creatinine clearance multiplied by f_p), renal secretion ($CL'_{sec,k}$ = geometric mean CL_R − mean $CL_{filtration}$) and the plasma hepatic (median CL_H) clearances of each renal impairment group were normalized to the corresponding value of the control group (Supplemental Table 2). These fractional changes were then incorporated into the rivaroxaban model to simulate

$$\frac{CL'_{int,H(+Erythromycin)}}{CL'_{int,H}} = \frac{f_{m,CYP3A}}{(K_{deg,CYP3A} + K_{obs,CYP3A})/K_{deg,CYP3A}} + \frac{f_{m,CYP2J2}}{1 + [I]/K_{i,CYP2J2}} + f_{m,non-CYP} \tag{7}$$

Copyright © 2012 John Wiley & Sons, Ltd.

DOI: 10.1002/bdd

Table 3. Change in rivaroxaban exposure relative to combined CYP3A4/P-gp inhibition and renal impairment. Note the simulated *AUC* ratio between the elderly and the young subjects is 1.3

Scenario	AUC_R of Rivaroxaban			
Observed [55](mean age 52 years)			CL_{cr} (ml/min)	
		50–80	30–49	15–29
- Erythromycin	1.0	1.4	1.5	1.6
+ Erythromycin	1.3			
			Renal impairment	
Simulated	Control	Mild	Moderate	Severe
Scenario 1[a] Younger population (20–45 years)				
- Erythromycin	1.0	1.6	1.9	2.1
+ Erythromycin	1.2	1.9	2.4	2.6
Scenario 2[b] Older population (55–65 years)				
- Erythromycin	1.0	1.5	1.7	1.8
+ Erythromycin	1.2	1.9	2.2	2.3
Scenario 3[c] Older population (55–65 years)				
- Erythromycin	1.3	2.0	2.2	2.3
+ Erythromycin	1.6	2.5	2.9	3.0

[a]Compared with younger control population not taking erythromycin.
[b]Compared with older control population not taking erythromycin.
[c]Compared with younger control population not taking erythromycin.

the effect of varying degrees of renal impairment – mild, moderate and severe, on rivaroxaban pharmacokinetics. In addition, it was assumed that RI has no effect on drug disposition of erythromycin. The validity of this assumption is unknown.

Creation of virtual populations to assess the effect of age on rivaroxaban exposure

Cross-study comparisons show that old patients appeared to have a lower clearance of rivaroxaban. Table 1 in Supplemental Material shows that the geometric mean values of CL/F were in the range 8–8.5 l/h for 51 years and older subjects [6,21]. Over a similar dose range (10–30 mg), CL/F values were 9.8–17.4 l/h for those younger than 45 years [5,11,22,23]. Therefore, the effect of age on rivaroxaban exposure was considered in the PBPK model. This was accomplished by incorporating age related changes into the PBPK model. First, two virtual populations, younger subjects (20–45 years) and older subjects (55–65 years), were created using SimCYP® software (Version 10.0). The 'Healthy volunteer population' of the software has an age range of 18–65 years. Using the 'Trial Design' function in SimCYP®, one can define the specific age range, numbers of subjects and proportion of females for a study population. Because a pre-defined demographic database (including central tendency and variability of known system-dependent parameters) has been compiled from the literature [24], demographic information of each study subject can be generated according to the Monte-Carlo approach. For each age group, 100 subjects were used. The GFR values were calculated based on the Cockcroft and Gault method [25]. The geometric means of body weight and GFR were calculated for each age group. These values were used to adjust the differences in CL_R according to Equation (6) and V_{ss}, respectively. Second, the values of CL_H, CL_R and $CL'_{sec,K}$ were adjusted for the older group. This was accomplished by calculating the differences in mean total CL and CL_R between the young healthy volunteers and those reported in the study in the older age group, assuming the rivaroxaban PK is the same between the virtual older group of this simulation and the subjects studied clinically. System- and drug-dependent parameters other than those specified above were assumed unchanged between the two age groups. Finally, these clearance terms were incorporated into the PBPK model to simulate the rivoxaban PK in these two age groups. For erythromycin, only V_{ss} was adjusted based on body weight differences between the two age groups. Other parameters remain unchanged between the two groups.

The main purpose of creating virtual populations was to generate system parameters for two

Copyright © 2012 John Wiley & Sons, Ltd.

DOI: 10.1002/bdd

distinct age groups (young and older) according to a pre-defined demographic database that has been compiled by SimCYP®. Note a relatively narrow age range for the older group (55–65 years) was used in this study, which was limited by the maximum age in the 'Healthy Volunteer Population' in SimCYP® (65 years). Also, simulations comparing these two age groups (see below) assumed that system-dependent parameters such as blood flows, tissue compositions, and enzyme abundance remained unchanged. Whereas SimCYP® output indicated that system-dependent parameters are different by >10% between the young and the older groups (data not shown). Therefore, the assumption that the disposition processes for both rivaroxaban and erythromycin remain unchanged with age may not be valid.

Simulation scenarios and data analyses

The PBPK models used in this study were constructed using SAAMII software (SAAM Institute, University of Washington, Seattle, WA, USA). The models were used to simulate rivaroxaban PK according to the following sequence: (1) in healthy subjects in the absence of an inhibitor [11]; (2) in healthy subjects in the presence of CYP3A4/P-gp inhibition by erythromycin [2–4,9] (3) in subjects with varying degrees of renal impairment [21], and (4) in subjects with varying degrees of renal impairment taking erythromycin. For scenario (3) and (4), simulations were conducted in both young and older virtual subjects. The simulation study designs (i.e. dose administration sequence and timing) were similar to those reported from the actual clinical studies. Erythromycin 500 mg was dosed three times daily for 4 days (total of 12 doses) in healthy subjects and in subjects with RI set as 25%, 50%, 75% and 90% of the baseline GFR. On day 4, a single oral dose of rivaroxaban was co-administered with the 10th dose of erythromycin.

Using the PBPK model developed for rivaroxaban, the simulated pharmacokinetic profile was compared with observed data from healthy subjects taking a 10 mg oral dose. The simulated profile reasonably describes the observed data reported by Kubitza and colleagues based on a visual analysis (Supplemental Figure 1). Because the PBPK model directly used systemic clearance from the *in vivo* study, the plot was only intended to show that the model, which incorporates more detailed drug elimination mechanisms by the liver and the kidney, is able to describe the rivaroxaban PK profile in humans.

The SAAMII simulated PK profiles were analysed by noncompartmental analysis using WinNonlin (V5.2, Pharsight Corp., Mountain View, CA, USA) to estimate the values of area under the concentration–time curve (*AUC*) for each of the four scenarios tested. The *AUC* ratios (*AUCR*) were calculated for scenarios 2–4 according to the equation below:

$$AUCR = \frac{AUC_i}{AUC_0}$$

AUC_i is the *AUC* under the condition of interference of drug disposition by intrinsic and/or extrinsic patient factors, and AUC_0 is the *AUC* of healthy subjects taking rivaroxaban only. For scenarios (3) and (4), *AUCR* values were calculated using the AUC_0 within each age group (i.e. young or older).

Results

Simulation of rivaroxaban pharmacokinetics in the presence of erythromycin

The PBPK model developed for erythromycin utilized time-dependent CYP3A4 inhibition and reversible CYP2J2 and P-gp inhibition to estimate a rivaroxaban *AUCR* of 1.20, whereas the observed *AUCR* was 1.34 (Table 3, subjects with normal renal function) [2–4,9].

Simulation of rivaroxaban pharmacokinetics in subjects with varying degrees of renal impairment (RI)

The estimated *AUCR* values within the young subjects appear to slightly over-predict the effect of renal impairment (1.6, 1.9, 2.1 compared with 1.4, 1.5, 1.6 for mild, moderate and severe RI, respectively, Table 3). The estimated *AUCR* values for older subjects (1.5, 1.7, and 1.8) according to the PBPK model are closer to the reported exposure changes of rivaroxaban in the published RI study. This is likely because the mean age of the

Copyright © 2012 John Wiley & Sons, Ltd.

DOI: 10.1002/bdd

subjects enrolled in the study was approximately 52 years [21].

Simulation of rivaroxaban pharmacokinetics in subjects with varying degrees of renal impairment and CYP3A4/P-gp inhibition

The simulated *AUCR* values of rivaroxaban in subjects with normal renal function and in subjects with varying degrees of renal impairments with and without co-administration with erythromycin are shown for each age group in Table 3 (Scenarios (1) and (2)). With any degree of renal impairment, the estimated *AUCR* following the concurrent use of erythromycin in both young and older subjects was greater than the effect by each individual factor alone.

It is important to note that the simulated exposures of Scenarios (1) and (2) (Table 3) are relative to the normal renal function subjects without co-medication within the particular age group. In fact, exposure simulations for the older subjects (Table 3 Scenario (3)) were approximately 30% higher than those for the younger group suggesting the elderly population may be at even greater risk if this complex DDI scenario exists.

Discussion

A complex DDI scenario exists when several different factors (e.g. renal impairment, hepatic impairment, metabolic enzyme inhibition, etc.) are considered, each alone does not cause a clinically relevant change in drug exposure, but they can result in a clinically relevant change when combined [26]. A key concern with this scenario is that, under certain conditions, this complex DDI can be synergistic leading to increases in drug exposure greater than the effect of either factor alone. The multifaceted nature of the complex DDI makes accurate quantification of the effect on exposure challenging and dedicated clinical studies are often not included in a drug application for approval. The absence of quantitative information creates a regulatory and clinical dilemma since it is almost impossible to optimize the dose in response to these scenarios and regulators are left with restriction through cautionary language.

It would be ideal if complex DDIs could be identified early in drug development so that clinical studies could be planned or prioritized to assess the risk. Unfortunately, in most cases, only *in vitro* and limited clinical data are available early in development. This makes such an assessment of complex DDI a challenge using traditional pharmacokinetic modeling. The PBPK approach has experienced a resurgence recently due to the development of highly sophisticated, population-based PBPK modeling and simulation tools [27,28], which may be valuable to addressing complex DDI issues. This approach is grounded in basic human physiology and chemistry and recent achievements allow for scaling of early *in vitro* and animal data to create a platform for simulations in humans [28]. The PBPK approach simultaneously incorporates multiple underlying physiology changes, which is not readily explicit using a classical compartmental pharmacokinetic approach.

Simulations from this study suggest that potentially clinically relevant drug–drug–RI interactions may exist when a combined P-gp and moderate CYP3A4 inhibitor is used concurrently with rivaroxaban in a subject with mild to moderate renal impairment. The model estimates for rivaroxaban exposure changes (i.e., 2–3 fold increases) in varying degrees of RI with concurrent erythromycin use are similar to the degree seen with strong CYP3A4/P-gp inhibitors such as ketoconazole and ritonavir in subjects with normal renal functions (Figure 1). Therefore, these *AUCR* values are consistent with those deemed 'significant increases in rivaroxaban exposure [that] may increase bleeding risk' reported in the approved product labeling for rivaroxaban [2]. This is not obvious when considering individual results regarding concurrent combined P-gp and moderate inhibitor use with rivaroxaban or the use of rivaroxaban in subjects with mild to moderate renal impairment. This becomes more disconcerting when one considers the steep exposure safety curve for rivaroxaban [2], the incidence of mild to moderate renal impairment in the elderly (see next paragraph), and the drugs that could be used concurrently in this population (e.g. amiodarone, verapamil, diltiazem) also fit into the moderate CYP3A4/P-gp inhibitor category.

These results also illustrate the importance of understanding the effect of patient factors on drug

Copyright © 2012 John Wiley & Sons, Ltd.

DOI: 10.1002/bdd

exposure in the population commonly studied in drug development. The renal clearance of rivaroxaban was lower (55%) and the relative exposure was higher (40–50%) in the elderly population (60–76 years), as compared to a younger population (19–45 years). The average age of patients participating in the phase 3 studies for rivaroxaban was 64 years, but the drug interaction studies were completed in younger healthy volunteers [4–6,9,11,21]. Often, translation of knowledge gained from clinical pharmacokinetic studies in healthy young subjects to target populations that may differ significantly in age is not straightforward. If significantly reduced drug clearance already exists between the elderly and young groups, the effect of complex DDI in the elderly group may be more substantial. During model development it appeared necessary to consider the effect of age when evaluating changes in both CL_H and CL_R of rivaroxaban in subjects with renal impairment (Table 3).

Further clinical studies would be needed to confirm these simulations before they can be used to optimize dosing. However, these results did support the cautionary language regarding the potential for complex DDI in the US product information for rivaroxaban [2]. In addition, these simulations also played a role in FDA's decision to require holders of the approved drug application to conduct a post-marketing clinical study [2] to quantify the pharmacokinetic and pharmacodynamic effects of this complex DDI under Section 505(o)(3) of the Food Drug and Cosmetic Act.

Certain caveats and limitations of our PBPK approach should be mentioned. First, although the simulation presented in this manuscript generally serves its purpose of revealing the impact of concurrent patient factors on the exposure of rivaroxaban, the model should be updated when new information becomes available, and be expanded to include stochastic features to assess inter-individual variability when needed. Second, because the majority of the published studies included primarily male subjects, extrapolation of age effects for female subjects may require further evaluation. Third, although decreased metabolism in RI was incorporated into the model, this assumption was based on relatively few published reports regarding altered metabolic activity with RI [30–34]. Protein binding effects were not incorporated into this model. This was because, while there is clear information regarding the effect of renal impairment on binding proteins in plasma, the available observed data for rivaroxaban did not show an obvious binding effect [21]. Fourth, several assumptions made in the model require further scrutiny. With regard to DDI mechanisms, the reversible K_i of erythromycin against CYP2J2 was assumed to be as potent as that by ketoconazole [35] to represent the worst case scenario. P-gp was assumed to be solely responsible for the net renal secretion of rivaroxaban. A reversible K_i value derived from a study using a known P-gp substrate digoxin was used for erythromycin, despite a recent report of minimal impact on P-gp mediated rivaroxaban transport *in vitro* by erythromycin [10]. Further model verification is needed for erythromycin's inhibition mechanisms, including sensitivity/uncertainty analyses of inhibition parameters. With regard to the creation of age groups, the validity related to the assumptions such as unchanged blood flow, tissue composition and enzyme abundance with age, is unknown.

Despite the limitations described above, this study highlights the importance of considering complex DDI in clinical practice and the importance of evaluating the degree of exposure change of a substrate under various clinical scenarios including multiple impairments. This brings to light the potential for PBPK to be used to aid in decision making regarding the need to evaluate multiple factor scenarios early in drug development.

Acknowledgements

E.G.B. and K.S.P. participated in this study as part of a Sabbatical at the Office of Clinical Pharmacology, Office of Office of Translational Sciences, Center for Drug Evaluation and Research, U.S. Food and Drug Administration, Silver Spring, MD, USA between 2009 and 2010. We would like to thank the Medical Products Agency and University of Toronto for permitting participation in this study.

The authors have no financial interest in the development of rivaroxaban or the modeling software used in this project. The authors declare no competing financial interests.

Professor Amin Rostami-Hodjegan (University of Manchester, UK), Dr. Masoud Jamei (SimCYP Ltd,

Copyright © 2012 John Wiley & Sons, Ltd.

DOI: 10.1002/bdd

Sheffield, UK) and Dr. Christofer Tornoe (Novo Nordisk A/S, Bagsværd, Denmark) are acknowledged for their valuable input in the development of standard PBPK models. We also thank Dr. Karen Yeo (SimCYP Ltd, Sheffield, UK) for sharing drug-dependent parameter information for erythromycin.

References

1. Janssen Pharmaceuticals, Inc. XARELTO® (rivaroxaban) package insert. Titusville, NJ; 2011. http://www.xareltohcp.com/xarelto-prescribing-information.html 1-27-2012.
2. US FDA. Approval History, NDA 022406 Xarelto (rivaroxaban) 10 mg immediate release Tablets. http://www.accessdata.fda.gov/drugsatfda_docs/appletter/2011/022406s000ltr.pdfhttp://www.accessdata.fda.gov/drugsatfda_docs/appletter/2011/022406s000ltr.pdf.
3. European Medicines Agency. Summary of Product Characteristics or SPC: Xarelto. Accessed September 6, 2011. www.ema.europa.eu/docs/en_GB/document_library/EPAR_-_Product_Information/human/000944/WC500057108.
4. European Medicines Agency. CHMP Assessment Report: Xarelto. Accessed September 6, 2011. www.ema.europa.eu/docs/en_GB/document_library/EPAR_-_Public_assessment_report/human/000944/WC500057122.
5. Kubitza D, Becka M, Wensing G, Voith B, Zuehlsdorf M. Safety, pharmacodynamics, and pharmacokinetics of BAY 59–7939 – an oral, direct Factor Xa inhibitor – after multiple dosing in healthy male subjects. *Eur J Clin Pharmacol* 2005; **61**: 873–880.
6. Kubitza D, Becka M, Roth A, Mueck W. Dose-escalation study of the pharmacokinetics and pharmacodynamics of rivaroxaban in healthy elderly subjects. *Curr Med Res Opin* 2008; **24**: 2757–2765.
7. Lang D, Freudenberger C, Weinz C. *In vitro* metabolism of rivaroxaban, an oral, direct factor Xa inhibitor, in liver microsomes and hepatocytes of rats, dogs, and humans. *Drug Metab Dispos* 2009; **37**: 1046–1055.
8. Weinz C, Schwarz T, Kubitza D, Mueck W, Lang D. Metabolism and excretion of rivaroxaban, an oral, direct factor Xa inhibitor, in rats, dogs, and humans. *Drug Metab Dispos* 2009; **37**: 1056–1064.
9. US FDA. FDA Advisory Committee Briefing Document: Cardiovascular and Renal Drugs Advisory Committee. March 19, 2009: 220–34. www.fda.gov/downloads/AdvisoryCommittees/CommitteesMeetingMaterials/Drugs/CardiovascularandRenalDrugsAdvisoryCommittee/UCM181524.pdf 9-6-2011.
10. Gnoth MJ, Buetehorn U, Muenster U, Schwarz T, Sandmann S. *In vitro* and *in vivo* P-glycoprotein transport characteristics of rivaroxaban. *J Pharmacol Exp Ther* 2011; **338**: 372–380.
11. Kubitza D, Becka M, Voith B, Zuehlsdorf M, Wensing G. Safety, pharmacodynamics, and pharmacokinetics of single doses of BAY 59–7939, an oral, direct factor Xa inhibitor. *Clin Pharmacol Ther* 2005; **78**: 412–421.
12. Nestorov IA, Aarons LJ, Arundel PA, Rowland M. Lumping of whole-body physiologically based pharmacokinetic models. *J Pharmacokinet Biopharm* 1998; **26**: 21–46.
13. Kanamitsu S, Ito K, Green CE, Tyson CA, Shimada N, Sugiyama Y. Prediction of *in vivo* interaction between triazolam and erythromycin based on *in vitro* studies using human liver microsomes and recombinant human CYP3A4. *Pharm Res* 2000; **17**: 419–426.
14. Rowland YK, Jamei M, Yang J, Tucker GT, Rostami-Hodjegan A. Physiologically based mechanistic modelling to predict complex drug–drug interactions involving simultaneous competitive and time-dependent enzyme inhibition by parent compound and its metabolite in both liver and gut – the effect of diltiazem on the time-course of exposure to triazolam. *Eur J Pharm Sci* 2010; **39**: 298–309.
15. Yang J, Kjellsson M, Rostami-Hodjegan A, Tucker GT. The effects of dose staggering on metabolic drug–drug interactions. *Eur J Pharm Sci* 2003; **20**: 223–232.
16. Jamei M, Marciniak S, Feng K, Barnett A, Tucker G, Rostami-Hodjegan A. The Simcyp((R)) Population-based ADME Simulator. *Expert Opin Drug Metab Toxicol* 2009; **5**: 211–223.
17. Rostami-Hodjegan A, Tucker GT. Simulation and prediction of *in vivo* drug metabolism in human populations from *in vitro* data. *Nat Rev Drug Discov* 2007; **6**: 140–148.
18. Pang KS, Rowland M. Hepatic clearance of drugs. I. Theoretical considerations of a 'well-stirred' model and a 'parallel tube' model. Influence of hepatic blood flow, plasma and blood cell binding, and the hepatocellular enzymatic activity on hepatic drug clearance. *J Pharmacokinet Biopharm* 1977; **5**: 625–653.
19. Eberl S, Renner B, Neubert A, *et al*. Role of p-glycoprotein inhibition for drug interactions: evidence from *in vitro* and pharmacoepidemiological studies. *Clin Pharmacokinet* 2007; **46**: 1039–1049.
20. Kurihara A, Hagihara K, Kazui M, Ozeki T, Farid NA, Ikeda T. *In vitro* metabolism of antiplatelet agent clopidogrel: cytochrome P450 isoforms responsible for two oxidation steps involved in the active metabolite formation. *Drug Metab Rev* 2005; **37**(Suppl 2): 99.
21. Kubitza D, Becka M, Mueck W, *et al*. Effects of renal impairment on the pharmacokinetics, pharmacodynamics and safety of rivaroxaban, an oral, direct Factor Xa inhibitor. *Br J Clin Pharmacol* 2010; **70**: 703–712.

Copyright © 2012 John Wiley & Sons, Ltd.

22. Kubitza D, Becka M, Zuehlsdorf M, Mueck W. Effect of food, an antacid, and the H2 antagonist ranitidine on the absorption of BAY 59–7939 (rivaroxaban), an oral, direct factor Xa inhibitor, in healthy subjects. *J Clin Pharmacol* 2006; **46**: 549–558.
23. Kubitza D, Becka M, Mueck W, Zuehlsdorf M. Rivaroxaban (BAY 59–7939) – an oral, direct Factor Xa inhibitor – has no clinically relevant interaction with naproxen. *Br J Clin Pharmacol* 2007; **63**: 469–476.
24. Jamei M, Dickinson GL, Rostami-Hodjegan A. A framework for assessing inter-individual variability in pharmacokinetics using virtual human populations and integrating general knowledge of physical chemistry, biology, anatomy, physiology and genetics: A tale of 'bottom-up' vs 'top-down' recognition of covariates. *Drug Metab Pharmacokinet* 2009; **24**: 53–75.
25. Cockcroft DW, Gault MH. Prediction of creatinine clearance from serum creatinine. *Nephron* 1976; **16**: 31–41.
26. Zhao P, Zhang L, Huang SM. Complex drug interactions: significance and evaluation. In *Enzyme- and Transporter-Based Drug-Drug Interactions: Progress and Future Challenges*. Pang KS, Rodrigus AD, Peter RM (eds). Springer: New York, 2010; 667–692.
27. Aarons L. Physiologically based pharmacokinetic modelling: a sound mechanistic basis is needed. *Br J Clin Pharmacol* 2005; **60**: 581–583.
28. Rowland M, Peck C, Tucker G. Physiologically-based pharmacokinetics in drug development and regulatory science. *Annu Rev Pharmacol Toxicol* 2011; **51**: 45–73.
29. Zhao P, Zhang L, Grillo JA, *et al*. Applications of physiologically based pharmacokinetic (PBPK) modeling and simulation during regulatory review. *Clin Pharmacol Ther* 2011; **89**: 259–267.
30. Dreisbach AW, Lertora JJ. The effect of chronic renal failure on drug metabolism and transport. *Expert Opin Drug Metab Toxicol* 2008; **4**: 1065–1074.
31. Nolin TD, Naud J, Leblond FA, Pichette V. Emerging evidence of the impact of kidney disease on drug metabolism and transport. *Clin Pharmacol Ther* 2008; **83**: 898–903.
32. Nolin TD. Altered nonrenal drug clearance in ESRD. *Curr Opin Nephrol Hypertens* 2008; **17**: 555–559.
33. Yeo KR, Aarabi M, Jamei M, Rostami-Hodjegan A. Modelling and predicting drug pharmacokinetics in patients with renal impairment. *Expert Opin Clin Pharmacol* 2011; **4**: 261–274.
34. Zhao P, Vieira M de LT, Grillo JA, *et al*. Evaluation of exposure change of non-renally eliminated drugs in patients with chronic kidney disease using physiologically-based pharmacokinetic modeling and simulation. *J Clin Pharmacol* 2012; **52**: 91S–108S.
35. Jones JP, Katayama JH, Jiang Y, Lee CA, Totah RA. Identification of danazol as a selective inhibitor of cytochrome P450 2J2. 15th North American regional meeting of International Society for the Study of Xenobiotics, October, 2008, San Diego, CA, USA.
36. Wang YH. Confidence assessment of the Simcyp time-based approach and a static mathematical model in predicting clinical drug–drug interactions for mechanism-based CYP3A inhibitors. *Drug Metab Dispos* 2010; **38**: 1094–1104.
37. Xu L, Chen Y, Pan Y, Skiles GL, Shou M. Prediction of human drug–drug interactions from time-dependent inactivation of CYP3A4 in primary hepatocytes using a population-based simulator. *Drug Metab Dispos* 2009; **37**: 2330–2339.
38. Dette GA, Knothe H, Herrmann G. Erythromycin binding to human serum. *Biochem Pharmacol* 1982; **31**: 1081–1087.
39. Austin KL, Mather LE, Philpot CR, McDonald PJ. Intersubject and dose-related variability after intravenous administration of erythromycin. *Br J Clin Pharmacol* 1980; **10**: 273–279.
40. Barre J, Mallat A, Rosenbaum J, *et al*. Pharmacokinetics of erythromycin in patients with severe cirrhosis. Respective influence of decreased serum binding and impaired liver metabolic capacity. *Br J Clin Pharmacol* 1987; **23**: 753–757.
41. Josefsson K, Bergan T, Magni L. Dose-related pharmacokinetics after oral administration of a new formulation of erythromycin base. *Br J Clin Pharmacol* 1982; **13**: 685–691.

Copyright © 2012 John Wiley & Sons, Ltd.

DOI: 10.1002/bdd